IAES International Journal of Artificial Intelligence (IJ-AI)
Vol. 5, No. 2, June 2016, pp. 45~54
ISSN: 2252-8938

Automatic Exudates Detection in Diabetic Retinopathy Images

H. Faouzi, M. Fakir
Information and processing teams, Faculty of Sciences and Technics, Sultan Moulay Slimane University,Morocco

Article Info

Article history:

Received Mar 2, 2016
Revised May 6, 2016
Accepted May 23, 2016

Keyword:

Detection
Diabetic Retinopathy
Fuzzy c-means
Gipt descriptors
Neural network.

ABSTRACT

Diabetic Retinopathy (DR) refers to the presence of typical retinal micro vascular lesions in persons with diabetics. When the disease is at the early state, a prompt diagnosis may help in preventing irreversible damages to the diabetic eye. If the exudates are closer to macula, then the situation is critical. Early detection can potentially reduce the risk of blind. This paper proposes tool for the early detection of Diabetic Retinopathy using edge detection, algorithm kmeans in segmentation phase, invariant moments (Hu and Affine) and descriptor GIST in extraction phase. In the recognition phase, neural network is adopted. All tests are applied on database DIARETDB1.

Corresponding Author:

H. Faouzi,
Information and processing teams,
Faculty of Sciences and Technics,
Sultan Moulay Slimane University,
Email: info.dec07@yahoo.fr

1. INTRODUCTION

Retinal image analysis is an essential step in the diagnosis of various eye diseases. Diabetic retinopathy is a complication of diabetes that is caused by changes in the blood vessels of the retina. The symptoms can blur or distort the patient's vision and are a main cause of blindness. Exudates are one of the primary signs of diabetic retinopathy. Medical Image Segmentation is the process of automatic or semi-automatic detection of boundaries within a 2D or 3D image. Image Segmentation is a process for dividing a given image into meaningful regions with homogeneous properties. A major difficulty of medical image segmentation is the high variability in medical images. The techniques presented in this paper can be classified into three categories: assessment and improvement of the image quality, segmentation of exudates and recognition [2,3,5].

2. PRE PROCESSING

After the acquisition of the image, recognition system begins with the pre-processing method comprising the following functions:

2.1. Choosing a Color Space

The color of our database images are acquired in the RGB space [4]. We can perform the treatment in this space. This approach has the advantage of ensuring data integrity, but it has a number of disadvantages among which the same color can be made quite differently by two screens. We can then look for a more appropriate space. The treatment is performed in the new space (after a transformation T), and the application of the inverse transformation (T-1, if it exists) is used, if necessary, for return to the RGB space (Figure 1).

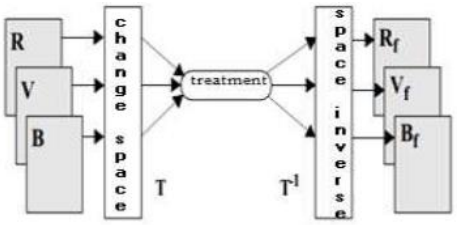

Figure 1. Treatment after projection in a suitable work space

2.2. RGB to HSI Space

HSI Color Model Hue, Saturation and Intensity are three important descriptors used by human being in describing colors. For example when we describe the color of retina or other object we never say that how red, green or blue the retina will be. Instead we describe the face in term of the brightness, the color, and also how dark or light the color will be. This is exactly what HSI color space do where H stands for hue will define the color, S stands for saturation will define how strong that particular color will be and I the intensities which specified the brightness. To separate the color components with intensity and brightness, the component retinal input images in the RGB color space are converted to the HSI color space (Figure 2).

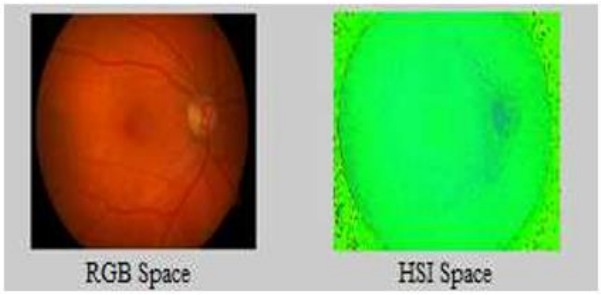

Figure 2. RGB to HSI space

2.3. Median Filtering

Median filtering is a nonlinear process useful in reducing impulsive or salt-and-pepper noise [1]. It is also useful in preserving edges in an image while reducing random noise. The median is calculated by first sorting all the pixel values from the surrounding neighborhood into numerical order and then replacing the pixel being considered with the middle pixel value. To evenly distribute the intensity of our database of images, the component I of the HSI color space is extracted and filtered through a 3x3 median filter (Figure 3).

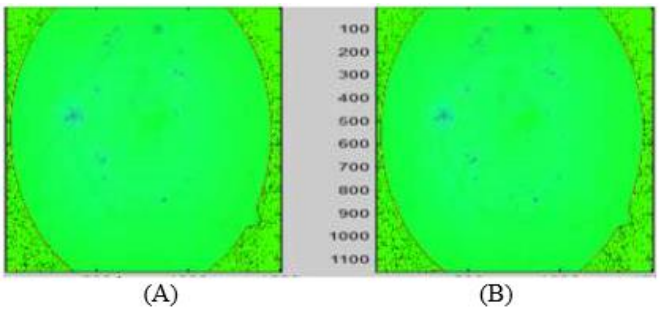

Figure 3. (A) Original image (B) Result of median filtering

2.4. Contrast-Limited Adaptive Histogram Equalization (CLAHE)

We used the Contrast-Limited Adaptive Histogram Equalization (CLAHE) [1] because it can increase the contrast between contours. The Contrast-Limited Adaptive Histogram Equalization is applied to component I of our filtered picture (Figure 4).

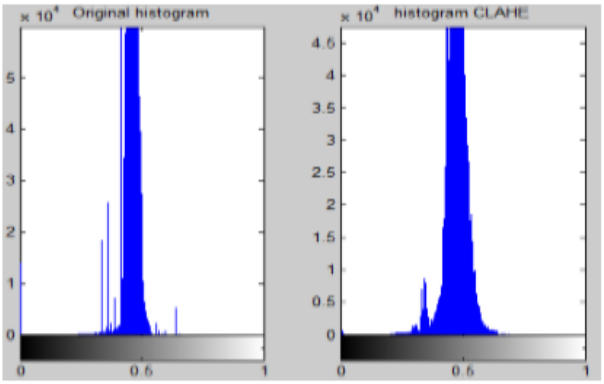

Figure 4. Contrast-Limited Adaptive Histogram Equalization

Figure 5. Final Image After Pre-Processing

3. SEGMENTATION

By definition, in image processing, segmentation is conventionally defined as the step of partitioning an image into homogeneous regions or zones. A region is then defined as a set of pixels that share a common characteristic such as intensity, color, texture.

3.1. Contour Segmentation

An Edge in an image is a significant local change in the image intensity, usually associated with a discontinuity in either the image intensity or the first derivative of the image intensity. The different edge detection methods used are Sobel, Prewitt, Roberts, Canny, LoG, EM algorithm, OSTU algorithm [8] and Genetic Algorithm. The prewitt operator is an approximate way to estimate the magnitude and orientation of the edge. The convolution mask of prewitt operator is shown in figure 6.

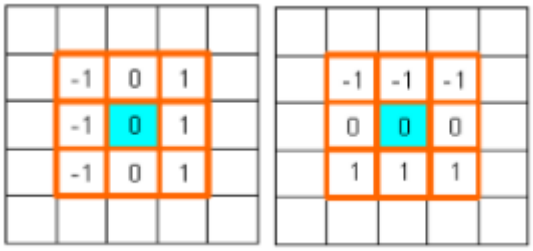

Figure 6. Mask of Prewitt Operator

Applying this filter to the pretreated in the preprocessing picture we get the result shown in Figure 7.

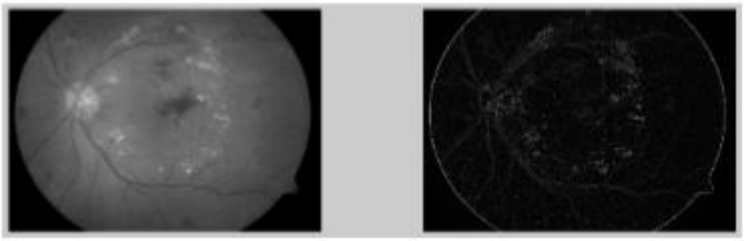

Figure 7. (A) Grayscale image (B) Result Prewitt filter

Laplacian filters are derivative filters used to find areas of rapid change (edges) in images. Since derivative filters are very sensitive to noise, it is common to smooth the image (e.g., using a Gaussian filter) before applying the Laplacian. This two-step process is called the Laplacian of Gaussian (LoG) operation.

$$\mathbf{L(x,y)} = \frac{\partial^2 \mathbf{I}}{\partial \mathbf{x}^2} + \frac{\partial^2 \mathbf{I}}{\partial \mathbf{y}^2} \quad (1)$$

The input image is represented as a set of discrete pixels; we need to find a discrete convolution kernel that can approximate the second derivatives in the definition of the Laplacian. Three kernels commonly used are shown in the Figure 8:

0	1	0
1	−4	1
0	1	0

1	1	1
1	−8	1
1	1	1

1	2	1
2	4	2
−1	2	−1

Figure 8. Discrete Convolution Kernel Approximate the Laplacian

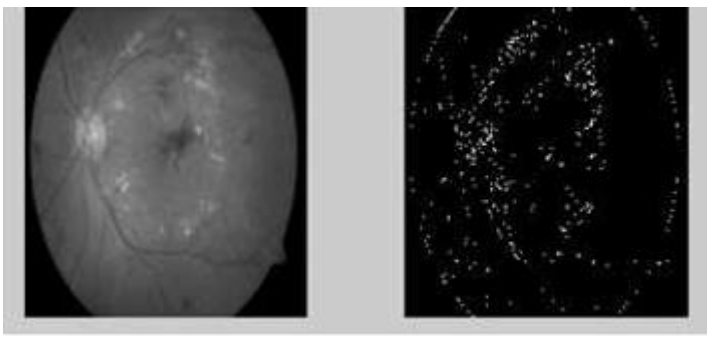

Figure 9. Laplacian of Gaussian Method

3.2. Region Based Segmentation

Region growing is a simple region segmentation method. It is also classified as a pixel based image segmentation method since it involves the selection of initial seed points. This approach to segmentation examines neighboring pixels of initial "seed points" and determines whether the pixel neighbors should be added to the region. The process is iterated on, in the same manner as general data clustering algorithms.

In this section, we present the segmentation based on the color characteristics of the image. The work is divided into two stages: First, we will improve the color of the image by extracting the components a

* b * of space L * a * b * [2]. Second the image will be grouping into a set of five groups using the k means algorithm. The whole process can be summarized in the following steps:

3.3. Converting the Image of the RGB Color Space to the CIE L * a * b

The CIE L * a * b * helps us to classify the color difference because the differences between these colors are closer to human perception.

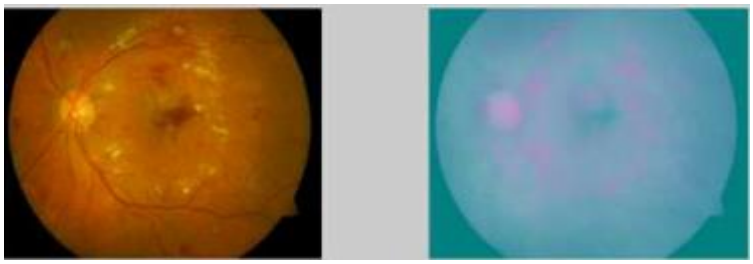

Figure 10. Converting the image of the RGB color space to the CIE L * a * b

3.4. Color Segmentation Using K-means Algorithm

The K-means algorithm [6] processes each object as having a location in space. The algorithm requires that we specifying the number of regions to be partitioned and a distance metric for quantifying the similarity between two pixels. In this phase we used the K-means algorithm to group pixels into five groups by using the Euclidean distance as the metric. Based on the result of this algorithm, we will label each pixel of the image with her cluster index.

3.5. Creating Images From Segments

In this step we will create images from segments we obtained the previous stage. The result the following Figure (Figure11).

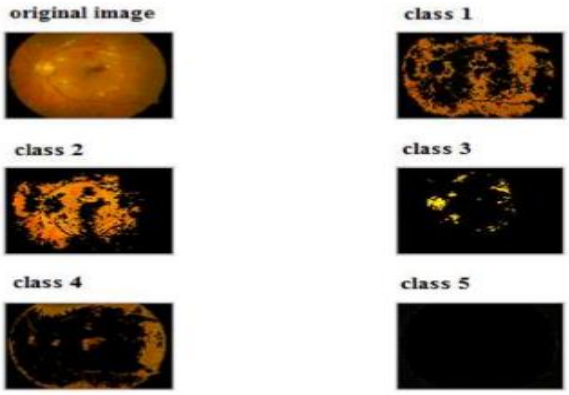

Figure 11. Results of the K-means algorithm

3.6. Selection and Binarization of Candidate Image

In this section, we will select and binarized the image candidate knowing that the optical disc and exudates are homogeneous in them color property and are characterized by a strong and brightness contrast comparable to other image. The result is indicated in the following Figure 12.

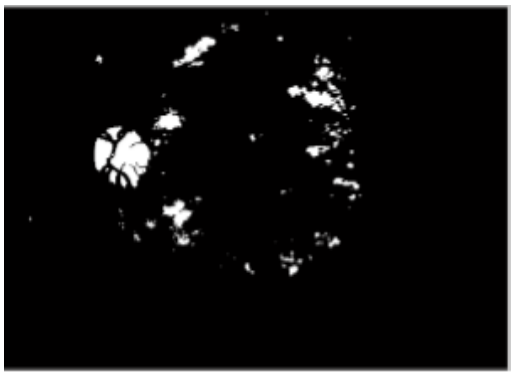

Figure 12. Final Segmentation Result of Optical Disc and Exudat

4. RECOGNITION OF EXUDAT

Exudates is first described by a set of invariant moments (Hu and Affine) and descriptor GIST then used in the stages of learning and recognition.The representation of images is an important step in the recognition phase. It must be invariant to geometric transformations (rotation, translation and scale factor) and robust to various disturbances (noise, dimming, etc). The representation we have adopted in this project is based on affine moment, Hu moment and GIST applied to binary images.

4.1. Moment Invariants [7]

The moments can be used to describe a form globally. Cartesian 2d moment invariant of order p, q for function f (x, y) is represented by:

$$\mathbf{m_{pq}} \int_{-\infty}^{+\infty} \int_{-\infty}^{+\infty} \mathbf{x^p y^q f(x,y) dxdy} \quad (2)$$

for a discrete image:

$$\mathbf{m_{pq}} = \sum_{\mathbf{x}} \sum_{\mathbf{y}} \mathbf{x^p y^q f(x,y)} \quad (3)$$

It is thus possible to calculate the moment order 0 represents the mass or area of a function:

$$\mathbf{m_{00}} = \sum_{\mathbf{x}} \sum_{\mathbf{y}} \mathbf{f(x,y)} \quad (4)$$

The two moments of order 1 are related to the corresponding coordinates of the center of the function:

$$\mathbf{m_{10}} = \sum_{\mathbf{x}} \sum_{\mathbf{y}} \mathbf{x\, f(x,y)} \quad (5)$$

$$\mathbf{m_{01}} = \sum_{\mathbf{x}} \sum_{\mathbf{y}} \mathbf{y\, f(x,y)} \quad (6)$$

From the two moments of order 1, we can find the center of mass of the form $(\overline{\mathbf{x}}, \overline{\mathbf{y}})$

$$(\overline{\mathbf{x}}, \overline{\mathbf{y}}) = (\frac{\mathbf{m_{10}}}{\mathbf{m_{00}}}, \frac{\mathbf{m_{01}}}{\mathbf{m_{00}}}) \quad (7)$$

The central moments can be expressed by:

$$\mu_{\mathbf{pq}} = \iint_{\mathbf{R}} (\mathbf{x} - \overline{\mathbf{x}})^{\mathbf{p}} (\mathbf{y} - \overline{\mathbf{y}})^{\mathbf{q}} \mathbf{f(x,y)} \quad (8)$$

For a digital image, the equation becomes:

$$\mu_{pq} = \sum_x \sum_y (x - \overline{x})^p \, (y - \overline{y})^q f(x, y) \tag{9}$$

4.2. Affine Moment

The affine transform is general linear transformation of space coordinates of the image:

$$x' = a_0 + a_1 x + a_2 y \tag{10}$$

$$y' = b_0 + b_1 x + b_2 y \tag{11}$$

The affine moment invariants are features for pattern recognition computed from moments of objects on images that do not change their value in affine transformation. In this work we will use the seven affine moments:

$$I_1 = (\mu_{20}\mu_{02} - \mu_{11}^2)/\mu_{00}^4$$

$$I_2 = (-\mu_{30}^2\mu_{03}^2 + 6\mu_{30}\mu_{21}\mu_{12}\mu_{03} - 4\mu_{30}\mu_{12}^3 - 4\mu_{21}^3\mu_{03} + 3\mu_{21}^2\mu_{12}^2)/\mu_{00}^{10}$$

$$I_3 = (\mu_{20}\mu_{21}\mu_{12}\mu_{03} - \mu_{20}\mu_{12}^2 - \mu_{11}\mu_{30}\mu_{03} + \mu_{11}\mu_{21}\mu_{12} + \mu_{02}\mu_{30}\mu_{12} - \mu_{02}\mu_{21}^2)/\mu_{00}^7$$

$$I_4 = (-\mu_{20}^3\mu_{03}^2 + 6\mu_{20}^2\mu_{11}\mu_{12}\mu_{03} - 3\mu_{20}^2\mu_{02}\mu_{12}^2 - 6\mu_{20}\mu_{11}^2\mu_{21}\mu_{03} - 6\mu_{20}\mu_{11}^2\mu_{12}^2 + 12\mu_{20}\mu_{11}\mu_{02}\mu_{21}\mu_{12} - 3\mu_{20}\mu_{02}^2\mu_{21}^2 + 2\mu_{11}^3\mu_{30}\mu_{03} + 6\mu_{11}^2\mu_{02}\mu_{30}\mu_{12} - 6\mu_{11}^2\mu_{02}\mu_{30}\mu_{12} - 6\mu_{11}^2\mu_{02}\mu_{21}^2 + 6\mu_{11}\mu_{02}^2\mu_{30}\mu_{21} - \mu_{02}^3\mu_{30}^2)/\mu_{00}^{11}$$

$$I_5 = (\mu_{40}\mu_{04} - 4\mu_{31}\mu_{13} + 3\mu_{22}^2/\mu_{00}^6$$

$$I_6 = (\mu_{40}\mu_{22}\mu_{04} - \mu_{40}\mu_{13}^2 - \mu_{31}^2\mu_{04} + 2\mu_{31}\mu_{22}\mu_{13} - \mu_{22}^3)/\mu_{00}^9$$

$$I_7 = \mu_{20}^2\mu_{04} - 4\mu_{20}\mu_{11}\mu_{13} + 2\mu_{20}\mu_{02}\mu_{22} + 4\mu_{11}^2\mu_{22} - 4\mu_{11}\mu_{20}\mu_{31} + \mu_{02}^2\mu_{40})/\mu_{00}^7 \tag{12}$$

4.3. Hu Moment

Based on normalized central moments, Hu introduced seven moment invariants:

$$\emptyset_1 = \mu_{20} + \mu_{02}$$

$$\emptyset_2 = (\mu_{20} - \mu_{02})^2 + 4\mu_{11}^2$$

$$\emptyset_3 = (\mu_{30} - 3\mu_{12})^2 + (3\mu_{21} - \mu_{03})^2$$

$$\emptyset_4 = (\mu_{30} + \mu_{12})^2 + (\mu_{21} + \mu_{03})^2 \tag{13}$$

$$\emptyset_5 = (\mu_{30} - 3\mu_{12})(\mu_{30} + \mu_{12})[(\mu_{30} + \mu_{12})^2 - 3(\mu_{21} + \mu_{03})^2] + (3\mu_{21} - \mu_{03})(\mu_{21} + \mu_{03})[3(\mu_{30} + \mu_{12})^2 - (\mu_{21} + \mu_{03})^2]$$

$$\emptyset_6 = (\mu_{20} - \mu_{02})[(\mu_{30} + \mu_{12})^2 - (\mu_{21} + \mu_{03})^2] + 4\mu_{11}(\mu_{30} + \mu_{12})(\mu_{21} + \mu_{03})$$

$$\emptyset_7 = (3\mu_{21} - \mu_{03})(\mu_{30} + \mu_{12})[(\mu_{30} + \mu_{12})^2 - 3(\mu_{21} + \mu_{03})^2] - (\mu_{30} - 3\mu_{12})(\mu_{21} + \mu_{03})[3(\mu_{30} + \mu_{12})^2 - (\mu_{21} + \mu_{03})^2]$$

The seven moment invariants are useful properties of being unchanged under image scaling, translation and rotation.

4.4. GIST Descriptors

In computer vision, GIST descriptors are a representation of an image in low dimension that contains enough information to identify the scene. Actually, any global descriptor must approach the GIST to be useful. GIST descriptor was proposed by Oliva and more precisely by Torralba [9]. They tried to capture the GIST descriptor of the image by analyzing the spatial frequencies and orientations.

4.5. Neural network construction

Figure 13 illustrate an example of neural network [10] used for the affine moment, namely a multilayer network that contains a hidden layer. In the following Table we summarise the decriptors with the number of neurons in input layer ,hidden layer and output layer.

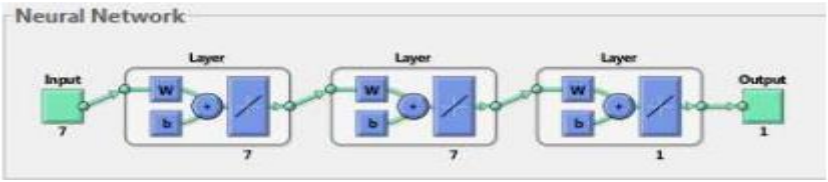

Figure 13. Structure of the neural network used for the affine moment.

Table 1. Construction of neural network for different descriptors

Descriptor	Number of neurons in input layer	Number of neurons in hidden layer	Number of neurons in output layer
Affine	7	7	1
Hu	8	8	1
GIST	512	512	1
Affine+HU	15	15	1
Affine+GIST	519	519	1
HU+GIST	520	520	1

5. RESULTS AND DISCUSSIONS

In order to interpret these results, we plotted several graphs (Figure 14, 15,16). These will allow us in particular to determine the best segmentation algorithm and the descriptor we will have to use. From graphs we constate that kmeans with Hu moment and GIST descriptors is bether than other decriptors in recognition rate.

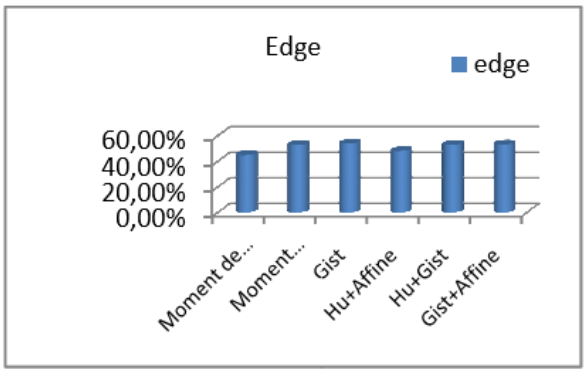

Figure 14. Result of segmentation by contour

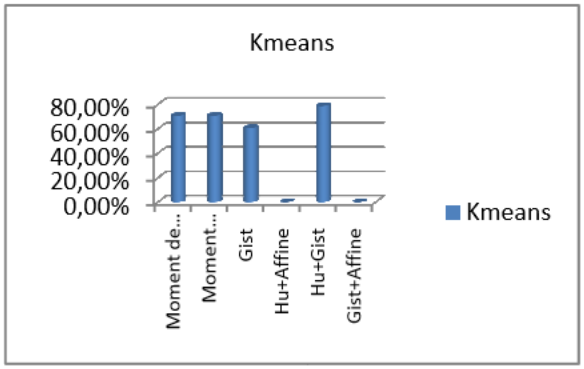

Figure 15. Result of segmentation by kmens

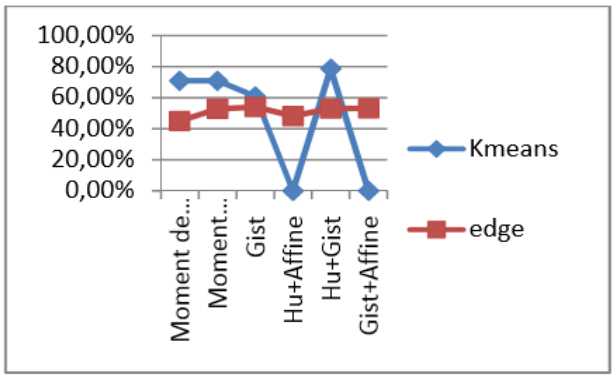

Figure 16. Comparison between methods

6. CONCLUSION

This study explored the issue of segmentation and recognition of exudates for diabetic retinopathy. We have presented two different parts two segmentation algorithms namely segmentation based on contour and k-means algorithm. For the extraction of characteristics of images w used Hu Moment, Affine Moment, GIST and different combination of these descriptors. To evaluate the performance of each algorithm on the detection of exudates, each descriptor was applied to the same set of images of an eye bottom and the results were compared. We confirmed in this study that kmeans segmentation algorithm appears to be more suited to the detection of exudates using Hu moments and GIST as a descriptoras a descriptor.

REFERENCES

[1] G Eason, B Noble, IN Sneddon. On Certain Integrals of Lipschitz-Hankel Type Involving Products of Bessel Functions. *Phil. Trans. Roy. Soc. London*. 1955; A 247: 529-551.
[2] JP Cocquerez, S Philipp. Analyse D.Image: Filtrage Et Segmentation. ed. Masson, 1995.
[3] Akara Sopharak, Khine Thet Nwe, Yin Aye Moe, Matthew N. Dailey et Bunyarit Uyyanonvara Automatic Exudate Detection with a Naive Bayes Classifier. Sirindhorn International Institute of Technology, Thammasat University & Computer Science and Information Management, Asian Institute of Technology.
[4] Alireza Osareh, Majid Mirmehdi, Barry Thomas, Richard Markham. *Classificationand localization of diabetic-related eye disease.* In Proc. of 7th European Conference on Computer Vision (ECCV). 2002: 502–516.
[5] Nichoals P, Ward, Stephen Tomlinson, et, Christopher J, Taylor. Image Analysis of Fundus Photographs: The detection and Measurement of Exudates Associated with Diabetic Retinopathy. Ophthalmology 1989; 96: 80-86.

[6] Alireza Osareh Majid Mirmehdi, Barry Thomas et Richard Markham. *Automatic Recognition of Exudative Maculopathy using Fuzzy C-Means Clustering and Neural Network*. Proc. Medical Image Understanding and Analysis Conference. Juillet 2001: 49-52.
[7] M-K Hu. Visual Pattern Recognition by Moment Invariant. IRE Trans Information Theory. 1962; 8:179–187.
[8] N Otsu. A Thresholding Selection Method from Gray Level Histograms. *IEEE Trans*. On syst, man and cybernetics, 1979, 9(1), 62-66.
[9] A Torralba, R Fergus, Y Weiss. Small codes and large databases for recognition. In CVPR, 2008.
[10] G Gardner, D Keating, T Williamson, et al. Automatic Detection of Diabetic Retinopathy Using an Artificial Neural Network: A Screening Tool. *British Journal of Ophthalmology*. 1996; 80: 940-944.
[11] A Frame, P Undrill, M Cree, et al. A Comparison of Computer Classification Methods Applied to Detection of Microaneurysms in Ophthalmic Fluorescein Angiograms. Computers in Biology and Medicine. 1998; 28: 225-238.